Crossref

creative commons

DOI: 10.31643/2025/6445.34
Engineering and Technology

Effect of substituting ZnO to ZnF_2 on Optical Properties of Nd^{3+}/Tm^{3+} Doped Tungsten-Bismuth-Tellurite Glass

[1]Farah Asyiqa A.Z.N., [1*]Yusof N.N., [1]Iskandar S.M., [2]Hisam R., [3]Azlan M.N., [4]Zaid M.H.M., [5]Abdul Hafidz Yusoff, [6]Nurulhuda M.Y.**

[1] Universiti Sains Malaysia, 11800 USM, Penang, Malaysia
[2] Universiti Teknologi MARA, 40450, Shah Alam, Selangor, Malaysia
[3] Sultan Idris Education University, 35900 Tajung Malim, Perak, Malaysia
[4] Universiti Putra Malaysia, 43400, UPM, Serdang, Selangor, Malaysia
[5] Universiti Malaysia Kelantan, Jeli Campus, 17600 Jeli, Kelantan, Malaysia
[6]Universiti Sultan Zainal Abidin, Gong Badak Campus, 21300 Kuala Nerus, Terengganu, Malaysia

** Corresponding author email: nurnabihah7@usm.my;*
*** Corresponding author email: nurulhudamy@unisza.edu.my*

Received: *May 10, 2024*
Peer-reviewed: *July 4, 2024*
Accepted: *August 29, 2024*

ABSTRACT

Present research explores the impact of varying ZnO and ZnF_2 concentrations in Nd^{3+}/Tm^{3+} doped Tungsten-Bismuth-Tellurite glass for fiber optic and solid-state application. Glasses with formula $60.97TeO_2–6.7WO_3–3.3\ Bi_2O_3–0.03Nd_2O_3–1TmO–(28-x)ZnO–xZnF_2$ where x = 0, 7, 14, 21, 28 mol% is prepared using melt-quenching technique. The absorption and photoluminescene of the glass is measured using a UV-Vis-NIR absorption and Photoluminescence spectrometer. About eight absorption bands are evidenced, centred around 467, 525, 581, 687, 726, 793, 870, 1211, and 1691 nm, corresponding to respective REIs (Nd^{3+} and Tm^{3+} ions) transitioning from the ground to their excited state. The absorbance of Tm^{3+} centred around 1691 nm improved with higher ZnF_2 contents (28% mol). Physical parameters such as density, molar volume, molar refractivity, and electronic polarizability are calculated. Seven prominent luminescence peaks of Nd^{3+} and Tm^{3+} have been identified centred around 509, 586, 611, 626, 648, 795, 800, and 890 nm. Highest luminescence enhancement is evident at 800 nm which corresponds to glass contained ratio of ZnO/ZnF_2 at 3:1. These findings highlight the role of ZnF_2 in altering the luminescence properties of the glass for fiber optics and solid-state laser applications.

Keywords: Zinc fluoride, tellurite glass, neodymium, thulium, rare-earth

Information about authors:

Nur Farah Asyiqa Abu Zaibidin — *Master's student at School of Physics, Universiti Sains Malaysia, 11800 USM, Penang, Malaysia. Email: farahasyiqa@student.usm.my; ORCID ID: https://orcid.org/0009-0008-5121-9308*

Nur Nabihah Yusof — *Dr., School of Physics, Universiti Sains Malaysia, 11800 USM, Penang, Malaysia. Email: nurnabihah7@usm.my; ORCID ID: https://orcid.org/0000-0002-6303-4908*

Iskandar Shahrim Mustafa — *Dr., School of Physics, Universiti Sains Malaysia, 11800 USM, Penang, Malaysia. ORCID ID: https://orcid.org/0000-0003-3875-4943*

Hisam R. — *Dr., Faculty of Applied Science, Universiti Teknologi MARA, 40450, Shah Alam, Selangor, Malaysia. ORCID ID: https://orcid.org/0000-0002-9183-4988*

Muhammad Noorazlan — *Dr., Physics Department, Faculty of Science and Mathematics, Universiti Pendidikan Sultan Idris, Tanjung Malim, Perak, 35900, Malaysia. Email: azlanmn@fsmt.upsi.edu.my; ORCID ID: https://orcid.org/0000-0002-2792-4145*

Zaid M.H.M. — *Dr. Physics Department, Faculty of Science, Universiti Putra Malaysia, 43400, UPM, Serdang, Selangor, Malaysia. ORCID ID: https://orcid.org/0000-0001-6734-800X*

Abdul Hafidz Yusoff — *Dr.,Universiti Malaysia Kelantan, 17600 Jeli; Dr., Gold, Rare Earth & Material Technopreneurship Centre (GREAT) Faculty of Bioengineering and Technology Universiti Malaysia Kelantan. Jeli Campus, 17600 Jeli, Kelantan, Malaysia. ORCID ID: https://orcid.org/0000-0003-0229-886X*

Nurulhuda Mohammad Yusoff — *UniSZA Science and Medicine Foundation Centre, Universiti Sultan Zainal Abidin, Gong Badak Campus, 21300 Kuala Nerus, Terengganu, Malaysia. Email: nurulhudamy@unisza.edu.my; ORCID ID: https://orcid.org/0000-0001-8219-2920*

Introduction

The wavelength-division-multiplexing (WDM) system, employing glass that is drawn into optical fiber is experiencing exponential growth to meet demands of fast data transmission [1]. To avoid signal attenuation, new gain media with high emission cross-section, operated at NIR range could be advantages [2]. Rare earth ions (REIs) doped glass is prospective as fiber optic amplifier with possible of broad emission bands at NIR region [[3], [4]]. Specifically, neodymium (Nd^{3+}) ion and thulium (Tm^{3+}) ion-doped glass are excellent as co-doped ion where their luminescence functionalized in NIR

region (800- 2000 nm) [[2], [5], [6], [7]]. Other than REIs ions, selection of glass hosts is equally important to selected REIs in developing efficient optical fiber amplifiers [[8], [9]]. Among glass, tellurite glasses are attractive since they have lower phonon energy (~750 cm^{-1}) compared to silica glasses (~1100 cm^{-1}), and borate glasses (1300 cm^{-1}) [10]. Tellurite glasses also exhibit wide transmission region, high refractive index, high solubility of rare earth ions, good chemical and mechanical durability; making them excellent choice as replacement of new fiber optics host [[11], [12], [13], [14]].

Tellurite glass properties can be further improved by appropriate amount of glass modifier. Tungsten oxide (WO_3) and bismuth oxide (Bi_2O_3) are selected as modifiers in the glass system. WO_3 and Bi_2O_3 are favourable in this work due to their ability to improve the glass transition temperature, density and refractive index, chemical durability, and moisture resistance, also, reduce the non-radiative loses [[15], [16], [17], [18]]. Less common glass modifier such as ZnF_2 able to reduce the phonon energy, improve the transparency, reduce hydroxide-adverse effect, decrease hygroscopic nature, possess strong transmission, and able to lower transition temperature as incorporated into tellurite glass [[14], [19], [20], [21]]. The inclusions of ZnF_2 resulting in absorbance and luminescence enhancement due to non-bridging oxygens (NBOs) generation with high polarizability that facilitate REIs transitions [22]. ZnF_2 role could be depending on its concentration within the composition [23]. For example, oxyfluorotellurite glasses increase molar volume along ZnF_2 contents. Two ligand atoms of ZnF_2, as opposed to only one oxygen in ZnO, creates more spaces and volume. This also impact the density and refractive index of the glass in general [21]. Neethish et al., claim that the replacement of ZnF_2 from BaO resulted in the destruction of the glass network and a subsequent decrease the optical band gap [24]. A few glass systems containing fluoride-based modifier also reported elsewhere such as TeO_2-ZnO-ZnF_2 [19], TeO_2-ZnO-ZnF_2 [25], TeO_2-ZnF_2 [26] B_2O_3-ZnF_2 [[20], [27]], AlF_3-ZnF_2 [28], TeO_2-BaO-BaF_2 [29], TeO_2-ZnO-BaF_2 [30], and ZnO-B_2O_3-SiO_2-ZnF_2 [31]. These findings suggest it is possible to alter optical properties of the glass by varied ZnF_2 contents during preparation process. Here ZnF_2 can lowers water absorption and reduces the multiphoton relaxation, result in improved luminescence.

The current work examines the effect of modifying the ZnO/ZnF_2 ratio in REIs doped glass. The glass formula $60.97TeO_2$–$6.7WO_3$–$3.3Bi_2O_3$–$0.03Nd_2O_3$–$1Tm_2O_3$–(28-*x*)ZnO–*x*ZnF_2 is prepared using the melt-quenching technique, where *x* = 0, 7, 14, 21, 28 mol%. The physical parameter such as density, refractive index, molar volume, field strength, molar refractivity, electronic polarizability, and inter-nuclear properties is calculated. The optical band gap energy of the sample glasses was determined. The unusual photoluminescence curve, featuring Nd^{3+} and Tm^{3+} ion is presented. This research purposely examines the potential of ZnF_2 as a glass modifier for any possible advancement of rare earth ions (REIs) doped glass as fiber optic amplifiers.

Experimental part

Glasses with formula $60.97TeO_2$–$6.7WO_3$–$3.3Bi_2O_3$–$0.03Nd_2O_3$–$1Tm_2O_3$–(28-*x*)ZnO–*x*ZnF_2 where *x* = 0, 7, 14, 21, 28 mol% was prepared using melt-quenching technique. The samples were labelled as TBNdTmZnF0, TBNdTmZnF7, TBNdTmZnF14, TBNdTmZnF21, and TBNdTmZnF28. The compositions were weighed 6 g per batch by a precision electronic balance according to chemical composition as in Table 1. The raw constituent was combined in alumina crucible by using a spatula to obtain a homogenous mixture. The mixtures were then placed in a high temperature furnace at 900 ˚C for 45 minutes under dry environment while the stainless-steel mold was preheated to remove residual moisture. Afterwards, the molten was quickly poured into stainless-steel mold to lessen thermal stress, enhance mechanical strength and it was kept in the annealing furnace at 300 ˚C for 6 hours before the furnace was switched off to cool down to room temperature. The Archimedes' principle method was performed to measure the density of the prepared glasses with water as immersed solution. The refractive index for each glass was obtained by using the formula given by Dimitriv & Sakka. The absorbance was recorded by UV-Vis-NIR spectrophotometer of Shimadzu UV-3600 Plus in the range of 400-2000 nm. The fluorescence spectrum in the visible to near-infrared range was recorded by FlouroMax-4 spectrofluorometer of Horiba Instruments. The data obtained from the spectrophotometer is analysed in the OriginLab software to identify the absorbance and luminescence bands, as well as to evaluate the optical band gap energy using Tauc's plot.

Table 1 - Chemical composition of the 60.97TeO_2–6.7WO_3–3.3 Bi_2O_3–0.03Nd_2O_3–1Tm_2O_3–(28-*x*)ZnO–*x*ZnF_2 (where *x* = 0, 7, 14, 21, 28 mol%)

Constituent/Glass	TBNdTmZnF0	TBNdTmZnF7	TBNdTmZnF14	TBNdTmZnF21	TBNdTmZnF28
TeO_2	60.97	60.97	60.97	60.97	60.97
ZnO	28.00	21.00	14.00	7.00	0.00
WO_3	6.70	6.70	6.70	6.70	6.70
Bi_2O_3	3.30	3.30	3.30	3.30	3.30
ZnF_2	0.00	7.00	14.00	21.00	28.00
Nd_2O_3	0.03	0.03	0.03	0.03	0.03
Tm_2O_3	1.00	1.00	1.00	1.00	1.00
TeO_2	60.97	60.97	60.97	60.97	60.97

Results and Discussion

Physical properties

Figure 1 shows photograph of the prepared tungsten-bismuth-tellurite glasses. The glass samples are coded as TBNdTmZnF0, TBNdTmZnF7, TBNdTmZnF14, TBNdTmZnF21, and TBNdTmZnF28, respectively according to to ZnF_2 concentration. The colour of prepared glass shows no significant colour changes as the ZnO/ZnF_2 concentration ratio varied [[32], [33]]. Alshamari et al., also mention a use of TeO_2 instead of B_2O_3 cause the glass samples colour change to more transparent light yellow instead of colourless transparent glass [34]. This could be due to impurities or defect in the glass network, where it should be transparent in high TeO_2 purity [[34], [35]].

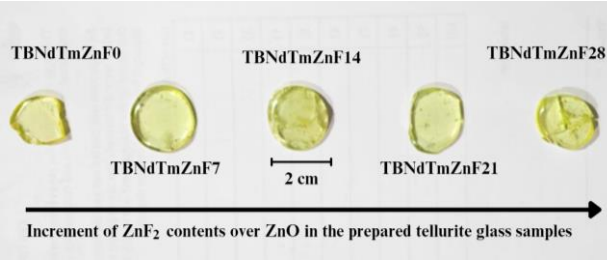

Figure 1 - As prepared Nd^{3+}/Tm^{3+} doped tungsten-bismuth-tellurite glasses with different ZnO/ZnF_2 ratio. The ZnF_2 contents (0.0-28.0 mol%) from left to right

The physical properties of Nd^{3+}/Tm^{3+} doped tellurite glasses are tabulated in Table 2 which the parameters are density, molar volume, refractive index, and polarizability is listed.

Figure **2** shows the (a) variation of density and molar volume also (b) refractive index and electronic polarizability of proposed glass. Archimedes' principle is utilized to compute the density, ρ, of the prepared glass [36].

$$\rho = \rho_w \frac{W_a}{W_a - W_w} \quad (2)$$

Where ρ_w, W_a, and W_w are density of distilled water (±0.997 g.cm^3) weight of the sample in the air, and weight of the sample in the distilled water respectively.

The density of the glass samples shows the fluctuated trend which varies from 5.718 to 5.8156 g/cm^3 but abruptly increases in TBNdTmZnF28 glass as compared to the other glass with ZnF_2 contents. There is distinct decrease in density between 7 and 21 mol% contributed two fluoride single bonds from ZnF_2 compared to ZnO with single double bond oxygen, leading to a network that is more voluminous and loosely-packed [31]. Smaller ionic radii of F^- (133 pm) compared to O^{2-} (140 pm) also could contribute to the decrement of the density in the glass, leaving more void in the system [37]. Nevertheless, the sudden increase of density from 21 to 28% elucidates a critical concentration where structure rearrangement could occur. At in this point, addition of ZnF_2 improves the compactness and make the network tightly packed. Here, the greater molecular weight of ZnF2 (103.39 g/mol) over ZnO (81.38 g/mol) intervenes, breaking the expected trend of density's reduction [[38], [39], [40], [41]]. The equation of molar volume of the glasses is calculated as following [36].

$$M_v = \frac{M}{\rho} \quad (2)$$

Where M_V represents the molar volume, M is the molecular weight, and ρ is the density of the samples. Molar volume, M_V, typically has contrary trend with density, ρ [[33], [42]]. Molar volume, M_V, shows the linear trend with addition of ZnF_2 that lies between 26.69 to 27.91 g/cm^3 from 0 to 21 mol%. According to Azuraida et al., the increase of the space in glass network increases the molar volume [[43], [44]]. In other words, ZnF_2 creates more void as it expands the inter-atom glass system [33]. However, the decrease trend is observed at glass contained 28 mol% of ZnF_2 (27.7225 g/cm^3). This might be caused structural rearrangement as the role converted from glass modifier to network as it exceeds 20 mol%, a common concentration limit for modifier in tellurite glass system. This in turn, tightens the glass network and makes it compact [44].

Table 2 - Density, molar volume, refractive index, and polarizability of the Nd^{3+}/Tm^{3+} doped tellurite glass

Glass	TBNdTmZnF0	TBNdTmZnF7	TBNdTmZnF14	TBNdTmZnF21	TBNdTmZnF28
Density (g/cm³)	5.81	5.82	5.77	5.72	5.81
Molar Volume (g/mol)	26.69	26.91	27.39	27.91	27.72
Refractive Index	1.924	1.926	1.929	1.925	1.960
Optical Band Gap Energy (eV)	3.20	3.18	3.16	3.19	2.94
Molar Refractivity (cm³/mol)	12.64	12.77	13.03	13.23	13.48
Polarizability ($\times 10^{-24}$ cm³)	5.81	5.82	5.77	5.72	5.81
Density (g/cm³)	26.69	26.91	27.39	27.91	27.72

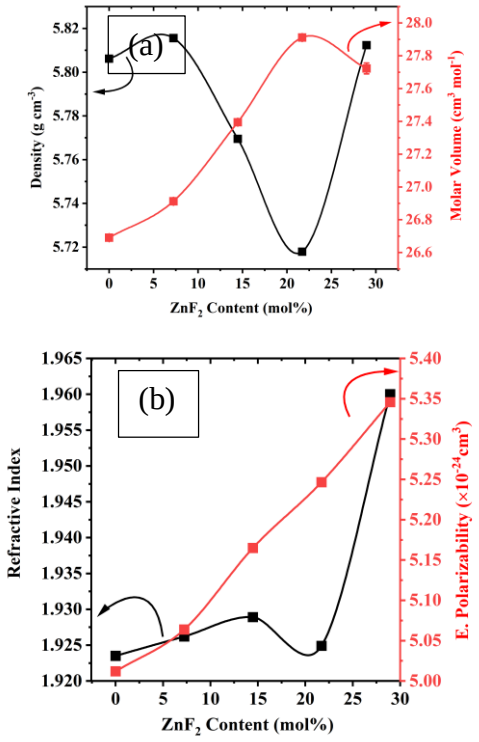

Figure 2 - Variation of (a) density and molar volume (b) refractive index and electronic polarizability with respect to the concentration of ZnF_2 in Nd^{3+}/Tm^{3+} doped tellurite glasses

The values of ionic concentration, N, inter-nuclear distance, r_i, polaron radius, r_p^2, and field strength, F of ZnF_2 for glass samples are listed in Table 3. The polaron radius, r_p, decreases from 0.75 to 0.48 Å as ZnF_2 increases into the glass, leads to the high field strength, F_S, from 5.37 to 13.26×10^{17} cm^{-2} around Zn^{2+} ions thus, contributes to the decrease in Zn-F_2 bond length and increase in Zn-F_2 bond strength [33]. Meanwhile, internuclear distance, r_i, decrease from 1.86 to 1.18 as ZnF_2 [45]. This parameter explains the reduction of molar volume, M_V, as well as the increment of density, ρ, as ZnF_2 reaches 28 mol% in the network. The similar pattern of the mentioned parameters is recorded in the previous studies as well [[46], [47], [48]]. The concentration of an ion, N, inter-nuclear distance, r_i, polaron radius, r_p^2, and field strength, F, are be obtained by the following equations [[46], [49]].

$$N = \text{mol\% of particular element} \times \frac{(N_A)(\rho)}{\text{glass average molecular mass}} \quad (3)$$

$$r_i = \left(\frac{1}{N}\right)^{\frac{1}{3}} \quad (4)$$

$$r_p = \frac{1}{2}\left(\frac{\pi}{6N}\right)^{\frac{1}{3}} \quad (5)$$

$$F = \frac{Z}{r_p^2} \quad (6)$$

where N_A is Avogadro's number, ρ is the density of the glass, and Z is the mass of the particular ion.

Table 3 - Ionic concentration, N, inter-nuclear distance, r_i, polaron radius, r_p^2, and field strength, F of ZnF_2 for each glass sample

Glass sample	Ionic concentration ($\times 10^{23}$ ions/cm³)	Inter-nuclear distance (Å)	Polaron radius (Å)	Field strength ($\times 10^{17}$ cm^{-2})
TBNdTmZnF0	-	-	-	-
TBNdTmZnF7	1.57	1.86	0.75	5.37
TBNdTmZnF14	3.08	1.48	0.60	8.42
TBNdTmZnF21	4.53	1.30	0.52	10.9
TBNdTmZnF28	6.08	1.18	0.48	13.26

Meanwhile, the refractive index increases from 1.936 to 1.984 along ZnF_2 contents. The refractive index is calculated by utilizing optical band gap energy, E_{opt} value through Dimitrov-Sakka equation [50].

$$\frac{n^2-1}{n^2+2}=1-\sqrt{\frac{E_{opt}}{20}} \quad (7)$$

where n is refractive index. E_{opt} is the optical band gap energy of the glass sample obtained by extrapolating linear part of the graph using Tauc's method. The absorption coefficient of the sample glasses is necessary to compute Tauc's plot. The following equations are absorption coefficient, α, from the absorption spectral data measured and also Tauc's relation [51].

$$\alpha=\frac{2.303A}{t} \quad (8)$$

$$\alpha=\frac{B\left(\hbar\upsilon-E_{opt}\right)^{r}}{\hbar\upsilon} \quad (9)$$

$$\alpha=B\exp\left(\frac{\hbar\upsilon}{E_{Urbach}}\right) \quad (10)$$

where A, t, B, and $\hbar\upsilon$ are absorbance, thickness of glass sample, independent constant which known as band tailing parameter, photon energy respectively. The index r =1/2, 3/2, 2, 3 represents direct allowed, direct forbidden, indirect allowed, and indirect forbidden transitions respectively [52]. Both allowed transition for direct and indirect of $(\alpha\hbar\upsilon)^{r}$ are plotted against $\hbar\upsilon$ to attain their respective optical band gap energy, E_{opt}, by extrapolating the slope on x-axis [42]. Whereas the Urbach energy, ΔE, is obtained by using the empirical relation in eq. (10), by calculating the reciprocal of the linear slope of In(α) against energy plot [18]. The direct, indirect optical band gap energy and Urbach energy decreases with increasing ZnF_2 from 3.11 to 2.78 eV, 3.20 to 2.94 eV, and from 0.35 to 0.33 cm^{-1}, respectively, as depicted in Table 3.

Figure **3** discloses Tauc's plot for sample coded TBNdTmZnF28, revealing extrapolated direct, indirect band gap and Urbach energy. The increase in Urbach energy indicates an increase in disorderliness with ZnF_2 inclusion within the glass.

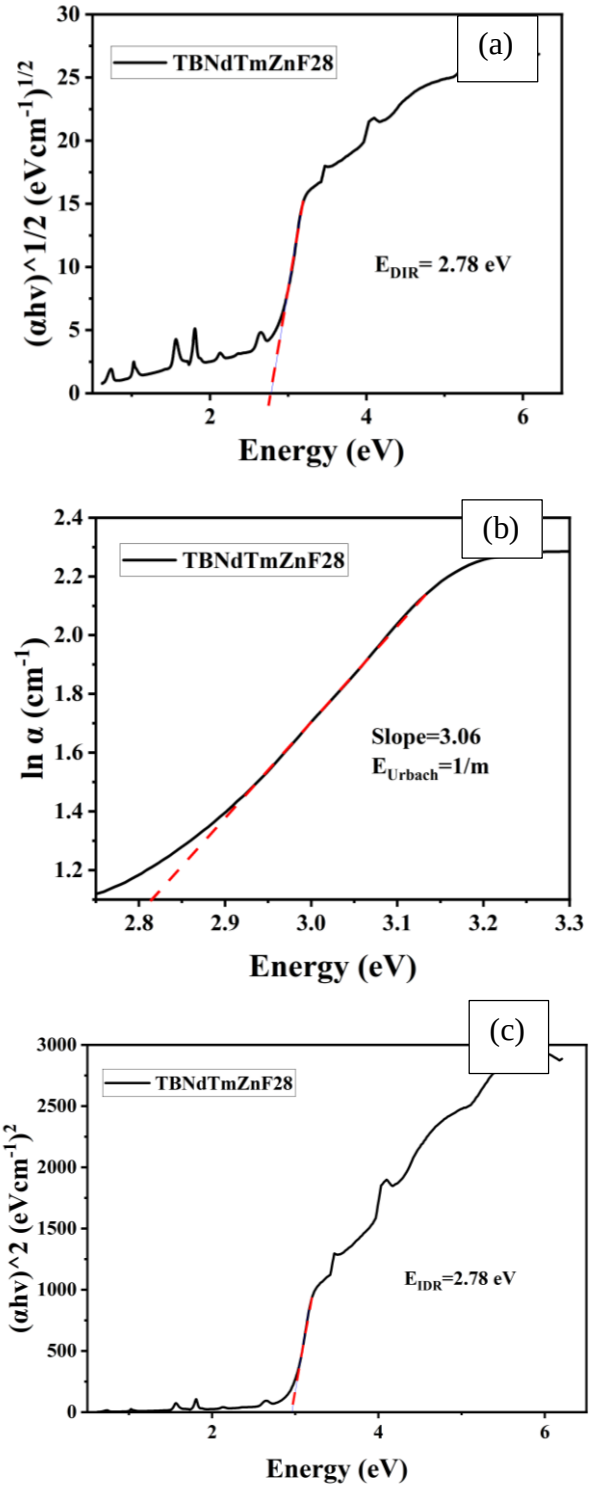

Figure 3 - (a) Direct energy band gap, (b) Indirect energy band gap, (c) Urbach energy of TBNdTmZnF28 glass

The refractive index possesses a direct relationship with the density, electric polarizability and the molecular electronic polarizability value is said to be consistent with the refractive index [41]. The electronic polarizability is one of the most important materials and it is closely related to their applicability in the field of optics and electronics

[38]. The trends refractive index and polarizability is portrayed in Table 2 and Figure 2. The polarizability of oxide and fluoride ions are computed the relation presented by Lorentz-Lorenz [53].

Table 4 - Direct energy band gap, indirect energy band gap, and Urbach energy of the Nd^{3+}/Tm^{3+} doped tellurite glasses

Constituent/Glass	TBNdTmZnF0	TBNdTmZnF7	TBNdTmZnF14	TBNdTmZnF21	TBNdTmZnF28
Direct Band Gap Energy (eV)	3.11	3.1	3.07	3.08	2.78
Indirect Band Gap Energy (eV)	3.20	3.18	3.16	3.19	2.94
Urbach Energy (cm^{-1})	0.35	0.28	0.20	0.18	0.33

$$\alpha_e = \left(\frac{3}{4\pi}\right)\left(\frac{R_m}{N_a}\right) \quad (11)$$

Where α_e is the electronic polarizability and R_m is the molar refractivity [42].

$$_M = \left(\frac{n^2-1}{n^2+2}\right)M_V \quad (12)$$

Furthermore, the loose packing of glass network from the high molar volume, M_V, happens to increase both molar refraction, R_m, and electronic polarizability, α_e, thus, explaining the increase of the refractive index, n [39]. The prior increase in molar refractivity, R_M, from 12.64 to 13.49 cm^3/mol may lead to the increase of the electronic polarizability with value of 5.01 to 5.35 $\times 10^{-24}$ cm^3. This might attribute to more polarizable non-bridging oxygens (NBOs) compared to the less polarizable bridging oxygens (BOs) [54]. According to Komal Poojha *et al.* higher polarizability is also attributed by anion with larger ionic radii which means fluorine (3.98) that is larger compared to oxygen (3.44) [[37], [55]]. It is worth mentioning that the linear relationship between n and ρ as mentioned in Gladstone-Dale equation is invalid for present work [56].

Absorption properties

Figure 4 shows the UV-vis-NIR absorption spectra of the range of 400-2000 nm of Nd^{3+}/Tm^{3+} doped tellurite glass samples. Eight absorption band is observed at 469, 527, 584, 697, 794, 868, 1212, and 1697 nm which originated from 4f-4f electronic transitions from the ground state $^4I_{9/2}$ of Nd^{3+} and $^3H_6$ of Tm^{3+} to their respective excited levels. To be specific, the wavelength peaks at 469, 527, 584, 697, 794, and 868 are belong to Nd^{3+} which the transitions from the ground state to $^4I_{9/2}$ to $^2K_{15/2}$+$^4G_{11/2}$, $^4G_{7/2}$, $^4G_{5/2}$, $^4F_{9/2}$, $^4F_{5/2}$, and $^4F_{3/2}$ excited levels. Whereas the wavelength peaks of Tm^{3+} at 469, 697, 794, 1212, and 1697 are assigned to the transitions from the ground state $^3H_6$ to $^1G_4$, $^3F_{2,3}$, $^3H_4$, $^3H_5$, and $^3F_4$ excited levels. The similar absorption bands have been reported in the previous studies with the doping of Nd^{3+}/Tm^{3+} ions into tellurite glass [[1], [57]]. However, there are a few of wavelength bands overlapped at the same wavelength which are at 469, 697, and 868 nm. The transitions in the UV-Visible region appear to be less intense compared to those transitions in NIR region due to the occurrence from the ground state of Nd^{3+}, $^4I_{9/2}$ to higher levels (^4G and ^4F) and from the ground state of Tm^{3+}, $^3H_6$ to higher levels (^3F) that are spin permissible, $(\Delta S = 0)$, except $^3H_6 \rightarrow {}^1G_4$ in Tm^{3+}, where $\Delta S = 2$ thus, it explains the weak absorption of the transition at wavelength 469 nm since the spin is forbidden. Moreover, major parts of these electronic transitions has been raised on account of induced electronic dipole transitions, complying with the selection rule, $|\Delta J| \leq 6$. Moreover, the transitions for Nd^{3+} from $^4I_{9/2}$ to $^2K_{15/2}$+$^4G_{11/2}$, $^4G_{7/2}$, and $^4F_{9/2}$ also for Tm^{3+}, $^3H_6$ to $^3H_5$ are marked as the allowed magnetic dipole transitions owing to $\Delta J = 0, \pm 1$. Furthermore, the $^3H_6 \rightarrow {}^3F_4$, $^3H_6 \rightarrow {}^3H_5$, and $^3H_6 \rightarrow {}^3H_4$ transitions of Tm^{3+} and $^4I_{9/2} \rightarrow {}^4F_{5/2}$ transition of Nd^{3+} are called named as hypersensitive transitions as they are very sensitive to the vicinity of the host and among the most intense than other transitions [[6], [58], [59]]. These transitions obey the selection rule, $|\Delta S| = 0$, $|\Delta L| \leq 2$, and $|\Delta J| \leq 2$.

However, the absorption peak assigned by - $^4I_{9/2} \rightarrow {}^4F_{9/2}$ exhibits the most intense, but forbidden by selection rules. The intensity of the individual absorption bands largely increases with the addition of ZnF_2 concentrations.

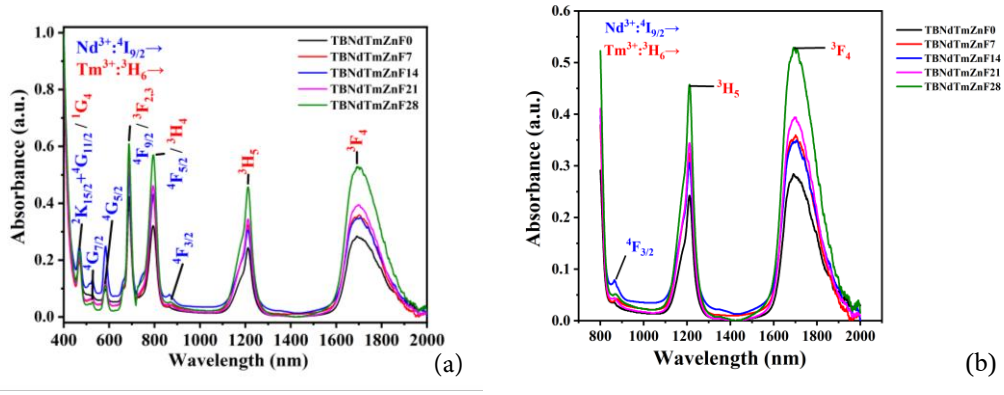

Figure 4 - Absorption spectra of (a) 400-2000 nm and (b) 800-2000 nm Nd^{3+}/Tm^{3+} doped tellurite glasses

Table 5 and Table 6 display the Nd^{3+} and Tm^{3+} ions doped tellurite glasses transition energies in wavelength number, λ (cm^{-1}), with the aquo-ion values. Major outcome of change in the characteristics of bonding between the Nd^{3+}/Tm^{3+} ions and neighbouring ligand ions (O^{2-}/F^{-}) in the host is attributed by the nephelauxetic effect [[49], [60]]. When the glass compositions in embedded with different modifiers in which also possess different charges, the band position will be varied since the ligands receive the charges from the central metal ion [55]. The nephelauxetic ratio is calculated as below [59].

$$\beta = \frac{\upsilon_B}{\upsilon_C} \qquad (13)$$

Where υ_B and υ_C are the wave number (cm^{-1}) of the corresponding transitions in the glass matric and aqua ion.

Nonetheless, bonding parameter values determine the nature of the bond between rare earth ions and their ligands (O^{2-}/F^{-}) are covalent or ionic depending on positive on the magnitude values. The formula for bonding parameter is as following [59].

$$\delta \left(\frac{1-\bar{\beta}}{\bar{\beta}}\right)\times 100 \qquad (14)$$

Where $\bar{\beta}$ is the average nephelauxetic ratio. The computed nephelauxetic ratio are 1.0917, 1.0911, 1.0912, 1.0926, and 1.0909 while the bonding parameters are -0.0840, -0.0835, -0.0836, -0.0848, and -0.0833 for glass samples TBNdTmZnF0, TBNdTmZnF7, TBNdTmZnF14, TBNdTmZnF21, and TBNdTmZnF28 respectively. The overall increase in nephelauxetic ratio also explains the shift to higher energy in absorption bands in Figure 4. As the nature of bonding between Nd^{3+}/Tm^{3+} ions and their ligands are ionic and consistent with the studied glasses [[49], [59], [60], [61]].

Table 5 - Calculated band positions (cm^{-1}), average nephelauxetic ratio ($\bar{\beta}$), bonding parameters (δ) of Nd^{3+} in aqua ion values in tellurite glasses

Energy level	TBNdTmZnF0	TBNdTmZnF7	TBNdTmZnF14	TBNdTmZnF21	TBNdTmZnF28	Aqua ion
$^4I_{9/2}\rightarrow{}^2K_{15/2}$ + $^4G_{11/2}$	21322	21322	21277	21322	21277	11527
$^4I_{9/2}\rightarrow{}^4G_{7/2}$	18939	18975	18939	18975	18975	12573
$^4I_{9/2}\rightarrow{}^4G_{5/2}$	17094	17094	17123	17123	17123	14854
$^4I_{9/2}\rightarrow{}^4F_{9/2}$	14556	14556	14556	14556	14556	17167
$^4I_{9/2}\rightarrow{}^4F_{5/2}$	12594	12594	12579	12610	12579	19103
$^4I_{9/2}\rightarrow{}^4F_{3/2}$	11561	11416	11561	11561	11455	21563
$\bar{\beta}$	1.0917	1.0911	1.0912	1.0926	1.0909	-
δ	-0.0840	-0.0835	-0.0836	-0.0848	-0.0833	-

Table 6 - Calculated band positions (cm^{-1}), average nephelauxetic ratio ($\bar{\beta}$), bonding parameters (δ) of Tm^{3+} in aqua ion values in tellurite glasses

Energy level	TBNdTmZnF0	TBNdTmZnF7	TBNdTmZnF14	TBNdTmZnF21	TBNdTmZnF28	Aqua ion
$^3H_6 \rightarrow {}^1G_4$	21322	21322	21277	21322	21277	5811.0000
$^3H_6 \rightarrow {}^3F_{2,3}$	14556	14556	14556	14556	14556	8390.0000
$^3H_6 \rightarrow {}^3H_4$	12594	12594	12579	12610	12579	12720.0000
$^3H_6 \rightarrow {}^3H_5$	8251	8258	8258	8251	8251	14510.0000
$^3H_6 \rightarrow {}^3F_4$	5914	5879	5865	5900	5914	21374.0000
$\bar{\beta}$	1.4479	1.4477	1.4458	1.4480	1.4461	-
δ	-0.3094	-0.3092	-0.3083	-0.3094	-0.3085	-

Photoluminescence Properties

The spectra in

Figure **5** shows the normalised ZnF_2 dependent PL emission spectra of all glass samples in the visible and partially near infrared range (500-900 nm) under the excitation wavelength of 467 nm at room temperature. Seven prominent luminescence peaks of Nd^{3+} and Tm^{3+} are identified centred around 509, 586, 611, 626, 648, 795, 800 and 890 nm which the transitions from excited states to ground states which are at $^4G_{9/2} \rightarrow {}^4I_{9/2}$, $^4G_{5/2} \rightarrow {}^4I_{9/2}$, $^2H_{11/2} \rightarrow {}^4I_{9/2}$, $^3F_3 \rightarrow {}^3H_6$, $^3H_4 \rightarrow {}^3H_6$, $^4F_{5/2} \rightarrow {}^4I_{9/2}$, and $^4F_{3/2} \rightarrow {}^4I_{9/2}$, respectively. The intensity and bandwidth of each spectrum are observed to be sensitive to ZnF_2 contents as they are varied. At wavelength 509 nm, the intensity of $^4G_{9/2} \rightarrow {}^4I_{9/2}$ transition increases up to 21 mol% ZnF_2. Nonetheless, it is noticed that the intensity of the transitions, $^4G_{5/2} \rightarrow {}^4I_{9/2}$, $^2H_{11/2} \rightarrow {}^4I_{9/2}$, and $^4F_{3/2} \rightarrow {}^4I_{9/2}$ at 586, 626, and 890 nm have been significantly decreasing with the presence of ZnF_2 concentration. Meanwhile, at the transitions of $^3F_3 \rightarrow {}^3H_6$, $^3H_4 \rightarrow {}^3H_6$, and $^4F_{5/2} \rightarrow {}^4I_{9/2}$ at wavelength 648, 795, and 800 nm, the luminescence intensity enhanced along with the addition of ZnF_2 content up to 7 mol% and later on the intensity decreases with further addition of ZnF_2 (≥ 14 mol%) contents, due to the phenomenon of concentration quenching [62]. The strongest luminescence intensity observed at 7 mol% of ZnF_2 which is the optimum concentration of ZnF_2 obtained in the present study. However, there are two emission bands of Nd^{3+} and Tm^{3+} partially overlapped and produced a wide luminescence spectrum at wavelength 795 and 800 nm.

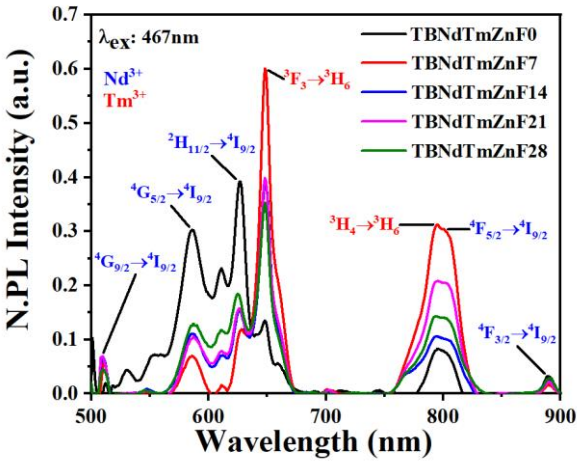

Figure 5 - Normalized PL spectra for all glass samples with the wavelength range of 500-900 nm

Figure 6 displays the partial energy diagram for the Nd^{3+}/Tm^{3+} ions, where non-radiative (NR) and radiative transitions are stipulated. In the presence of 467 nm excitation, the Nd^{3+} ions are promoted to the $^2D_{3/2}$, $^2P_{3/2}$ state while the Tm^{3+} ions are promoted to the $^1G_4$ state. Afterwards, the Nd^{3+}/Tm^{3+} ions went through multi-phonon relaxations processes and the lower states, particularly for Nd^{3+}, $^4G_{9/2}$, $^4G_{5/2}$, $^2H_{11/2}$, $^4F_{5/2}$, and $^4F^{3/2}$ while for Tm^{3+}, $^3F_3$ and $^3H_4$ are occupied. Green, orange, and red emissions are identified in Nd^{3+} ions while orange and red are detected in Tm^{3+}ions. The non-radiation transitions are attributed to the strong interaction among the respective Nd^{3+}/Tm^{3+} ions, as the distance between the ions decreases [39].

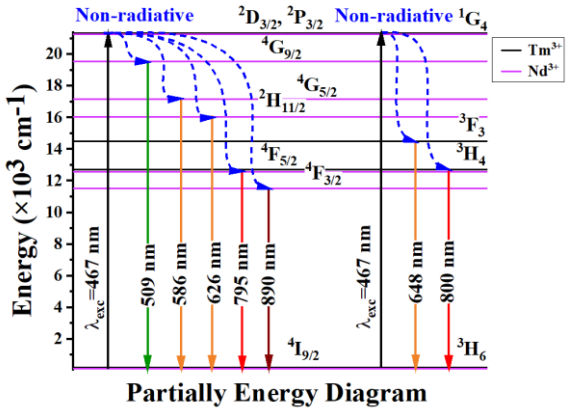

Figure 6 - Partially energy level diagram of Nd^{3+}/Tm^{3+} ions in TBNdTmZnF glasses

Conclusions

Varying the ZnO/ZnF_2 contents in Nd^{3+}/Tm^{3+} doped Tungsten-Bismuth-Tellurite glass demonstrate its substantial impact in physical and optical properties of prepared glass. The absorbance centred around 1691 nm, corresponding to Tm^{3+} ions improved with ZnF_2 contents. Physical parameters such as density, molar volume, molar refractivity, and electronic polarizability fluctuated at different ZnF_2 concentration. The changes in refractive index attributable to the polarizability differences between fluoride and oxygen anions. The prominent luminescence band is evidenced at 800 nm which highlighting the capable of ZnF_2 in tuning the luminescence properties which it shifts the wavelength towards NIR region. This work suggested that ZnF_2 can alter the optical properties of REIs doped glass, that is useful in develop better fiber optics and solid-state lasers materials operated at NIR region.

Conflicts of interest. On behalf of all authors, the corresponding author states that there is no conflict of interest.

CRediT author statement

A.Z.N. Farah Asyiqa: Conceptualization, Writing - Original Draft, Methodology, Formal analysis. **N.N.Yusof:** Conceptualization, Writing - Original Draft, Writing - Review & Editing, Funding acquisition, Supervision, Methodology**. S.M. Iskandar:** Writing - Review & Editing, Supervision, Methodology. **R. Hisam:** Writing - Review & Editing. **M.N. Azlan:** Writing - Review & Editing**. Zaid M.H.M.:** Writing - Review & Editing. **Abdul Hafidz Yusoff:** Writing - Review & Editing. **M.Y. Nurulhuda:** Writing - Review & Editing

Acknowledgements. The research was supported financially by Universiti Sains Malaysia through USM Short-Term Grant with Project No: 304/PFIZIK/6315739. We also appreciated financial support from International Kurita Grant with no: R504-LR-GAL008-0000000139-K120. The research work also was supported by UniSZA/2021/DPU1.0/21/R0325.

Cite this article as: Farah Asyiqa AZN, Yusof NN, Iskandar SM, Hisam R, Azlan MN, Zaid MHM, Abdul Hafidz Yusoff, Nurulhuda M.Y. Effect of substituting ZnO to ZnF_2 on Optical Properties of Nd^{3+}/Tm^{3+} Doped Tungsten-Bismuth-Tellurite Glass. Kompleksnoe Ispolzovanie Mineralnogo Syra = Complex Use of Mineral Resources. 2025; 335(4):5-17. https://doi.org/10.31643/2025/6445.34

ZnO-ны ZnF_2-ге ауыстырудың Nd^{3+}/Tm^{3+} легирленген Вольфрам-Висмут-Теллуритті әйнектің оптикалық қасиеттеріне әсері

[1]Farah Asyiqa A.Z.N., [1*]Yusof N.N., [1]Iskandar S.M., [2]Hisam R., [3]Azlan M.N., [4]Zaid M.H.M., [5]Abdul Hafidz Yusoff, [6]Nurulhuda M.Y.**

[1] Сайнс Малайзия Университеті, 11800 USM, Пенанг, Малайзия
[2]MARA технологиялық университеті, 40450, Шах Алам, Селангор, Малайзия
[3] Сұлтан Ыдырыс білім университеті, 35900 Таджунг Малим, Перак, Малайзия
[4] Малайзия Путра университеті, 43400, UPM, Серданг, Селангор, Малайзия
[5] Келантан Малайзия университеті, 17600 Джели, Келантан
[6]Сұлтан Зайнал Абидин университеті, Гонг Бадак кампусы, 21300 Куала Нерус, Теренгану, Малайзия

ТҮЙІНДЕМЕ

Зерттеу Nd^{3+}/Tm^{3+} легірленген вольфрам-висмут-теллуритті шынының әртүрлі ZnO және ZnF_2 концентрацияларының оптикалық-талшықты және қатты күйде қолдану үшін әсерін зерттейді. Формуласы $60,97TeO_2–6,7WO_3–3,3\ Bi_2O_3–0,03Nd_2O_3–1TmO–(28-x)ZnO–xZnF_2$ болатын шынылар (мұнда x = 0, 7, 14, 21, 28 моль%) балқыту әдісімен дайындалады. Шынының жұтылуы және фотолюминесценциясы UV-Vis-NIR жұтылу және

Мақала келді: *10 мамыр 2024*
Сараптамадан өтті: *4 шілде 2024*
Қабылданды: *29 тамыз 2024*

фотолюминесценция спектрометрінің көмегімен өлшенеді. 467, 525, 581, 687, 726, 793, 870, 1211 және 1691 нм орталықтарында сегізге жуық жұтылу жолақтары анықталған, бұл REI (Nd^{3+} және Tm^{3+} иондарының) негізгі күйден қозған күйге ауысқан күйлеріне сәйкес келеді. Орталығы 1691 нм болатын Tm^{3+} жұту қабілеті ZnF_2 мөлшері жоғары (28% моль) болғанда жақсарды. Тығыздық, молярлық көлем, молярлық сыну қабілеті және электронды поляризациялану сияқты физикалық параметрлер есептеледі. Nd^{3+} және Tm^{3+} жеті люминесценция шыңдарының 509, 586, 611, 626, 648, 795, 800 және 890 нм айналасында орналасқан. Люминесценцияның ең жоғары күшейуі 800 нм-де байқалады, бұл шыныдағы ZnO/ZnF_2 3:1 қатынасына сәйкес келеді. Бұл нәтижелер оптикалық талшықтар мен қатты күйдегі лазерлер үшін қолданылатын шынының люминесценттік қасиеттерін өзгертудегі ZnF_2 рөлін көрсетеді.

Түйінді сөздер: мырыш фториді, теллуритті шыны, неодим, тулий, сирек жер элементтері.

Авторлар туралы ақпарат:

Nur Farah Asyiqa Abu Zaibidin *Магистрант, Физика мектебі, Сайнс Малайзия Университеті, 11800 USM, Пенанг, Малайзия. Email: Farahasyiqa@student.usm.my; ORCID ID: https://orcid.org/0009-0008-5121-9308*

Nur Nabihah Yusof *PhD, Физика мектебі, Сайнс Малайзия Университеті, 11800 USM, Пенанг, Малайзия. Email: nurnabihah7@usm.my; ORCID ID: https://orcid.org/0000-0002-6303-4908*

Iskandar Shahrim Mustafa *PhD, Физика мектебі, Сайнс Малайзия Университеті, 11800 USM, Пенанг, Малайзия. ORCID ID: https://orcid.org/0000-0003-3875-4943*

Hisam R. *Доктор, қолданбалы ғылымдар факультеті, MARA технологиялық университеті, 40450, Шах Алам, Селангор, Малайзия. ORCID ID: https://orcid.org/0000-0002-9183-4988*

Muhammad Noorazlan *Сұлтан Ыдырыс атындағы білім университетінің жаратылыстану-математика факультеті физика кафедрасының докторы, Танджунг Малим, Перак, 35900, Малайзия. Email: azlanmn@fsmt.upsi.edu.my; ORCID ID: https://orcid.org/0000-0002-2792-4145*

Zaid M.H.M. *Доктор, Физика кафедрасы, ғылым факультеті, Малайзия Путра университеті, 43400, UPM, Serdang, Селангор, Малайзия. ORCID ID: https://orcid.org/0000-0001-6734-800X*

Abdul Hafidz Yusoff *PhD, Малайзия университеті Келантан, 17600 Джели; PhD, сирек жер және материалдар технологиясы кәсіпкерлік орталығы (GREAT), биоинженерия және технологиялар бөлімі, Малайзия университеті, Келантан. Джели кампусы, 17600 Джели, Келантан, Малайзия. ORCID ID: https://orcid.org/0000-0003-0229-886X*

Nurulhuda M.Y *Сұлтан Зайнал Абидин университеті, Гонг Бадак кампусы, 21300 Куала Нерус, Теренгану, Малайзия. ORCID ID: https://orcid.org/0000-0001-8219-2920*

Влияние замены ZnO на ZnF_2 на оптические свойства Вольфрам-Висмут-Теллуритового стекла, легированного Nd^{3+}/Tm^{3+}

[1]Farah Asyiqa A.Z.N., [1*]Yusof N.N., [1]Iskandar S.M., [2]Hisam R., [3]Azlan M.N., [4]Zaid M.H.M., [5]Abdul Hafidz Yusoff, [6]Nurulhuda M.Y.**

[1] Университет Сайнс Малайзия, 11800 USM, Пенанг, Малайзия
[2] Технологический университет MARA, 40450, Шах-Алам, Селангор, Малайзия
[3] Университет образования Султана Идриса, 35900 Таджунг Малим, Перак, Малайзия
[4] Университет Путра Малайзия, 43400, UPM, Серданг, Селангор, Малайзия
[5] Университет Малайзии Келантан, Кампус Джели, 17600 Джели, Келантан, Малайзия
[6]Университет Султана Зайнала Абидина, кампус Гонг Бадак, 21300 Куала Нерус, Теренгану, Малайзия

Поступила: *10 мая 2024*
Рецензирование: *4 июля 2024*
Принята в печать: *29 августа 2024*

АННОТАЦИЯ

Настоящее исследование изучает влияние различных концентраций ZnO и ZnF_2 в вольфрам-висмут-теллуритном стекле, легированном Nd^{3+}/Tm^{3+}, для применения в оптоволокне и полупроводниках. Стекла формулы $60{,}97TeO_2–6{,}7WO_3–3{,}3\ Bi_2O_3–0{,}03Nd_2O_3–1TmO–(28-x)ZnO–xZnF_2$, где x = 0, 7, 14, 21, 28 мол.%, получают методом закалки из расплава. Поглощение и фотолюминесценцию стекла измеряют с помощью спектрометра поглощения и фотолюминесценции UV-Vis-NIR. Выявлено около восьми полос поглощения с центрами около 467, 525, 581, 687, 726, 793, 870, 1211 и 1691 нм, соответствующих соответствующим РЗИ (ионам Nd^{3+} и Tm^{3+}), переходящим из основного в возбужденное состояние. Поглощение Tm^{3+} с центром около 1691 нм улучшалось при более высоком содержании ZnF_2 (28% мол.). Рассчитываются физические параметры, такие как плотность, молярный объем, молярная преломляющая способность и электронная поляризуемость. Были идентифицированы семь заметных пиков люминесценции Nd^{3+} и Tm^{3+}, сосредоточенных около 509, 586, 611, 626, 648, 795, 800 и 890 нм. Наибольшее усиление люминесценции наблюдается при длине волны 800 нм, что соответствует соотношению ZnO/ZnF_2 в стекле 3:1. Эти результаты подчеркивают роль ZnF_2 в изменении люминесцентных свойств стекла для волоконной оптики и твердотельных лазеров.

Ключевые слова: фторид цинка, теллуритное стекло, неодим, тулий, редкоземельные элементы.

Информация об авторах:

Nur Farah Asyiqa Abu Zaibidin *Магистрант, Школа физики, Университет Сайнс Малайзия, 11800 USM, Пенанг, Малайзия. Email: Farahasyiqa@student.usm.my; ORCID ID: https://orcid.org/0009-0008-5121-9308*

Nur Nabihah Yusof *Доктор философии, Школа физики, Университет Сайнс Малайзия, 11800 USM, Пенанг, Малайзия. Email: nurnabihah7@usm.my; ORCID ID: https://orcid.org/0000-0002-6303-4908*

Iskandar Shahrim Mustafa *Доктор философии, Школа физики, Университет Сайнс Малайзия, 11800 USM, Пенанг, Малайзия. ORCID ID: https://orcid.org/0000-0003-3875-4943*

Hisam R. *Доктор, факультет прикладных наук, Технологический университет MARA, 40450, Шах Алам, Селангор, Малайзия. ORCID ID: https://orcid.org/0000-0002-9183-4988*

Muhammad Noorazlan *Доктор кафедры физики факультета естественных наук и математики Образовательного университета Султана Идриса, Танджунг Малим, Перак, 35900, Малайзия. Email: azlanmn@fsmt.upsi.edu.my; ORCID ID: https://orcid.org/0000-0002-2792-4145*

Zaid M.H.M. *Доктор, кафедра физики, факультет естественных наук, Университет Путра Малайзия, 43400, UPM, Серданг, Селангор, Малайзия. ORCID ID: https://orcid.org/0000-0001-6734-800X*

Abdul Hafidz Yusoff *Доктор наук, Центр технологического предпринимательства редкоземельных металлов и материалов (GREAT), факультет биоинженерии и технологий Университета Малайзии, Кампус Джели, 17600 Джели, Келантан, Малайзия. ORCID ID: https://orcid.org/0000-0003-0229-886X*

Nurulhuda M.Y *Университет Султана Зайнала Абидина, кампус Гонг Бадак, 21300 Куала Нерус, Теренгану, Малайзия. ORCID ID: https://orcid.org/0000-0001-8219-2920*

References

[1] Xia L, Zhang Y, Ding J, Li C, Shen X, Zhou Y. $Er^{3+}/Tm^{3+}/Nd^{3+}$ tri-doping tellurite glass with ultra-wide NIR emission. Journal of Alloys and Compounds. 2021; 863:158626. https://doi.org/10.1016/j.jallcom.2021.158626

[2] Hou G, Cao L, Zhang C, et al. Improvement of ultra-broadband near-infrared emission in Nd^{3+}-Er^{3+}-Pr^{3+} tri-doped tellurite glasses. Optical Materials. 2021; 111:110547. https://doi.org/10.1016/j.optmat.2020.110547

[3] Kaniyarakkal S, Rajasekharaudayar KC, Dagupati R, et al. Down-/Up-conversion luminescence behaviors and energy transfer analysis in Tm^{3+} and Tm^{3+}/Yb^{3+} co-doped tellurite glasses. Inorganic Chemistry Communications. 2023; 158(P1):111395. https://doi.org/10.1016/j.inoche.2023.111395

[4] Elkhoshkhany N, Marzouk S, El–Sherbiny M, et al. Enhanced thermal stability and optical and structural properties of Tm^{+3} ions in doped tellurite glasses for photonic use. Results in Physics. 2021; 24:104202. https://doi.org/10.1016/j.rinp.2021.104202

[5] Song X, Han K, Zhou D, Xu P, Xue X, Zhang P. ~2 μm emission properties and energy transfer processes in Tm^{3+} doped Bi_2O_3-GeO_2-Na_2O glass laser material. Journal of Luminescence. 2020; 224:117314. https://doi.org/10.1016/j.jlumin.2020.117314

[6] Cao J, Xu P, Song C, et al. Realization of broadband ∼1.8 μm luminescence by level population inversion in Tm^{3+} doped tellurite glass for laser applications. Journal of Non-Crystalline Solids. 2023; 617:122445. https://doi.org/10.1016/j.jnoncrysol.2023.122445

[7] Lakshminarayana G, Meza-Rocha AN, Soriano-Romero O, et al. Survey of optical and fluorescence traits of Tm^{3+}-doped alkali/mixed alkali oxides constituting B_2O_3-BaO-ZnO-LiF glasses for 0.45 μm laser and 1.46 μm fiber amplifier. Results in Physics. 2021; 26:104343. https://doi.org/10.1016/j.rinp.2021.104343

[8] Zhao D, Zhu L, Li C, Ding J, Li J, Zhou Y. Broadband near-infrared luminescence property in Nd^{3+}/Tm^{3+} co-doped tellurite glass. Journal of Alloys and Compounds. 2023; 937:168384. https://doi.org/10.1016/j.jallcom.2022.168384

[9] Djamal M, Yuliantini L, Hidayat R, et al. Spectroscopic study of Nd3+ ion-doped Zn-Al-Ba borate glasses for NIR emitting device applications. Optical Materials. 2020; 107:110018. https://doi.org/10.1016/j.optmat.2020.110018

[10] Kumar A, Anu, Sahu MK, et al. Spectral characteristics of Tb^{3+} doped ZnF_2–K_2O–Al_2O_3–B_2O_3 glasses for epoxy free tricolor w-LEDs and visible green laser applications. Journal of Luminescence. 2022; 244:118676. https://doi.org/10.1016/j.jlumin.2021.118676

[11] Siva Rama Krishna Reddy K, Swapna K, Mahamuda S, Venkateswarulu M, Rao AS. Structural, optical and photoluminescence properties of alkaline-earth boro tellurite glasses doped with trivalent Neodymium for 1.06 μm optoelectronic devices. Optical Materials. 2021; 111:110615. https://doi.org/10.1016/j.optmat.2020.110615

[12] Feng S, Zhu J, Liu C, et al. The deactivation effects of Nd^{3+} ion for 2.85 μm laser in Ho^{3+}/Nd^{3+} co-doped fluorotellurite glass. Journal of Luminescence. 2024; 266:120308. https://doi.org/10.1016/j.jlumin.2023.120308

[13] Zhu L, Zhao D, Li C, Ding J, Li J, Zhou Y. Effect of Nb_2O_5 on the ∼2.0 μm band luminescence of $Ho^{3+}/Tm^{3+}/Ce^{3+}$ tri-doped tellurite glass. Ceramics International. 2023; 49(18):30490-30500. https://doi.org/10.1016/j.ceramint.2023.06.313

[14] Zhang C, Han K, Wu T, et al. TeO_2-GeO_2-BaF_2-Tm_2O_3 glass for ∼2 μm laser materials: Analysis of luminescence features and energy transfer behavior. Ceramics International. 2022; 48(20):30546-30554. https://doi.org/10.1016/j.ceramint.2022.06.335

[15] Li C, Zhang X, Onah VC, et al. Physical and optical properties of TeO_2-WO_3-GdF_3 tellurite glass system. Ceramics International. 2022; 48(9):12497-12505. https://doi.org/10.1016/j.ceramint.2022.01.116

[16] Biswas J, Jana S. Photoluminescence of Tb^{3+}/Sm^{3+} ions co-activated in SrO - Na_2O - WO_3 - tellurite glasses for multicolor laser applications. Ceramics International. 2023; 49(15):24718-24729. https://doi.org/10.1016/j.ceramint.2023.04.215

[17] Sayyed MI, D'Souza AN, Prabhu NS, Kamath SD. Comparing basic radiation attenuation factors of tellurite glasses containing $PbCl_2$ and Bi_2O_3 with some other potential glass systems. Optik. 2022; 249:168247. https://doi.org/10.1016/j.ijleo.2021.168247

[18] Prasad RNA, Venkata Siva B, Neeraja K, Krishna Mohan N, Rojas JI. Influence of modifier oxides on spectroscopic features of Nd_2O_3 doped PbO-Ro_2O_3–WO_3–B_2O_3 glasses (with Ro_2O_3 = Sb_2O_3, Al_2O_3, and Bi_2O_3). Journal of Luminescence. 2020; 223:117171. https://doi.org/10.1016/j.jlumin.2020.117171

[19] Gunha JV, Muniz RF, Somer A, et al. The effect of fluorine replacement on the physical properties of oxyfluorotellurite glasses TeO_2-Li_2O-ZnO-ZnF_2. Journal of Non-Crystalline Solids. 2023; 603:122083. https://doi.org/10.1016/j.jnoncrysol.2022.122083

[20] Rajesham S, Sekhar KC, Shareefuddin M, Kumar JS. Impact of MoO_3 on physical and spectroscopic (optical, FTIR, Raman and EPR) studies of B_2O_3-CdO-Al_2O_3-ZnF_2 glasses for optical and shielding applications. Optik. 2023; 272:170241. https://doi.org/10.1016/j.ijleo.2022.170241

[21] Sanju, Ravina, Anu, et al. Physical, structural and optical characterization of Dy^{3+} doped ZnF_2-WO_2-B_2O_3-TeO_2 glasses for opto-communication applications. Optical Materials. 2021; 114:110937. https://doi.org/10.1016/j.optmat.2021.110937

[22] Kilic G, Issever UG, Ilik E. Synthesis, characterization and crystalline phase studies of TeO_2–Ta_2O_5–ZnO/ZnF_2 oxyfluoride semiconducting glasses. Journal of Non-Crystalline Solids. 2020; 527:119747. https://doi.org/10.1016/j.jnoncrysol.2019.119747

[23] Ravina, Naveen, Sheetal, et al. Judd-Ofelt itemization and influence of energy transfer on Sm^{3+} ions activated B_2O_3–ZnF_2–SrO–SiO_2 glasses for orange-red emitting devices. Journal of Luminescence. 2021; 229:117651. https://doi.org/10.1016/j.jlumin.2020.117651

[24] Neethish MM, Acharyya JN, Prakash GV, Ravi Kanth Kumar V V. Effect of Zinc Fluoride addition on structure of barium Borate glasses for nonlinear optical applications. Optical Materials. 2021; 121:111626. https://doi.org/10.1016/j.optmat.2021.111626

[25] Gunha JV, Muniz RF, Somer A, et al. The effect of fluorine replacement on the physical properties of oxyfluorotellurite glasses TeO2-Li2O-ZnO-ZnF2. Journal of Non-Crystalline Solids. 2023; 603:122083. https://doi.org/10.1016/j.jnoncrysol.2022.122083

[26] Abd El-Moneim A. Effect of ZnF2 and WO3 on elastic properties of oxyfluoride tellurite ZnF_2–WO_3–TeO_2glasses: Theoretical analysis. Chinese Journal of Physics. 2020; 65:412-423. https://doi.org/10.1016/j.cjph.2020.02.013

[27] Nagaraju R, Sekhar KC, Shareefuddin M, Haritha L, Lalitha G, Kumar KV. Influence of ZnF_2/PbF_2 on physical and structural characteristics of bismuth borate glasses reinforced with chromium ions. Optik. 2021; 247:168028. https://doi.org/10.1016/j.ijleo.2021.168028

[28] Zhang C, Zhang C, Yun C, Lai S. 3.1 μm mid-infrared luminescence in Er^{3+} doped ZnF_2 modified aluminum fluoride glass. Journal of Rare Earths. 2023; 41(7):997-1003. https://doi.org/10.1016/j.jre.2022.09.021

[29] Yuan J, Wang W, Ye Y, et al. Effect of BaF_2 Variation on Spectroscopic Properties of Tm^{3+} Doped Gallium Tellurite Glasses for Efficient 2.0 μm Laser. Frontiers in Chemistry. 2021; 8:1-6. https://doi.org/10.3389/fchem.2020.628273

[30] Aishwarya K, Vinitha G, Varma GS, Asokan S, Manikandan N. Synthesis and characterization of barium fluoride substituted zinc tellurite glasses. Physica B: Condensed Matter. 2017; 526:84-88. https://doi.org/10.1016/j.physb.2017.09.039

[31] Kullberg ATG, Lopes AAS, Monteiro RCC. Effect of ZnF_2 addition on the crystallization behaviour of a zinc borosilicate glass. Journal of Non-Crystalline Solids. 2017; 468(May):100-104. https://doi.org/10.1016/j.jnoncrysol.2017.04.030

[32] Vahedigharehchopogh N, Kıbrıslı O, Ersundu AE, Çelikbilek Ersundu M. Color tunability and white light generation through up-conversion energy transfer in Yb^{3+} sensitized Ho^{3+}/Tm^{3+} doped tellurite glasses. Journal of Non-Crystalline Solids. 2019; 525:119679. https://doi.org/10.1016/j.jnoncrysol.2019.119679

[33] Ahmed AA, Mawlud SQ. Physical and optical properties of ternary lead-bismuth tellurite glass. Heliyon. 2023; 9(6):e16730. https://doi.org/10.1016/j.heliyon.2023.e16730

[34] Alshamari A, Mhareb MHA, Alonizan N, et al. Gamma-ray-induced changes in the radiation shielding, structural, mechanical, and optical properties of borate, tellurite, and borotellurite glass systems modified with barium and bismuth oxide. Optik. 2023; 281:170829. https://doi.org/10.1016/j.ijleo.2023.170829

[35] Baynton PL. Colour of tellurite glasses. Nature. 1955; 176(4484):691-692. https://doi.org/10.1038/176691b0

[36] Yuliantini L, Djamal M, Hidayat R, Boonin K, Kaewkhao J, Yasaka P. Luminescence and Judd-Ofelt analysis of Nd^{3+}ion doped oxyfluoride boro-tellurite glass for near-infrared laser application. Materials Today: Proceedings. 2018; 43:2655-2662. https://doi.org/10.1016/j.matpr.2020.04.631

[37] Shannon RD. Revised effective ionic radii and systematic studies of interatomic distances in halides and chalcogenides. Acta Crystallographica. 1976; 32(5):751-767. https://doi.org/10.1023/A:1018927109487

[38] Shoaib M, Khan I, Iskakova K, et al. Investigation of luminescence properties of Ho^{3+} doped barium, zinc and gadolinium based phosphate glasses. Optik. 2022; 260:169046. https://doi.org/10.1016/j.ijleo.2022.169046

[39] Kıbrıslı O, Ersundu AE, Ersundu MÇ. Dy $^{3+}$ doped tellurite glasses for solid-state lighting: An investigation through physical, thermal, structural and optical spectroscopy studies. Journal of Non-Crystalline Solids. 2019; 513:125-136. https://doi.org/10.1016/j.jnoncrysol.2019.03.020

[40] Anigrahawati P, Sahar MR, Sazali ES. Physical, structural and spectroscopic analysis of tellurite glass containing natural magnetite Fe_3O_4 nanoparticles. Materials Chemistry and Physics. 2022; 286:126183. https://doi.org/10.1016/j.matchemphys.2022.126183

[41] Shoaib M, Khan I, Chanthima N, et al. Photoluminescence analysis of Er^{3+}-ions Doped P_2O_5-Gd_2O_3/GdF_3-BaO-ZnO glass systems. Journal of Alloys and Compounds. 2022; 902:163766. https://doi.org/10.1016/j.jallcom.2022.163766

[42] Lenkennavar SK, Eraiah B, Kokila MK. Rare earths doped oxy-fluoride glasses as candidates for generating tunable visible light. Materials Today: Proceedings. 2020; 33:2550-2554. https://doi.org/10.1016/j.matpr.2019.12.066

[43] Azuraida A, Halimah MK, Sidek AA, et al. Comparative studies of bismuth and barium boro-tellurite glass system: Structural and optical properties. Chalcogenide Letters. 2015; 12(10):497-503.

[44] Adamu SB, Halimah MK, Chan KT, Muhammad FD, Nazrin SN, Tafida RA. Eu^{3+} ions doped zinc borotellurite glass system for white light laser application: Structural, physical, optical properties, and Judd-Ofelt theory. Journal of Luminescence. 2022; 250:119099. https://doi.org/10.1016/j.jlumin.2022.119099

[45] Kaur M, Singh A, Thakur V, Singh L. Thermal, optical and structural properties of Dy^{3+} doped sodium aluminophosphate glasses. Optical Materials. 2016; 53:181-189. https://doi.org/10.1016/j.optmat.2016.01.051

[46] Ali AA, Shaaban MH. Optical and Electrical Properties of Nd^{3+} Doped TeBiY Borate Glasses. Silicon. 2018; 10(4):1503-1511. https://doi.org/10.1007/s12633-017-9633-y

[47] Krishna VM, Mahamuda S, Rani PR, Swapna K, Venkateswarlu M, Rao AS. Effect of samarium ions concentration on physical,

optical and photoluminescence properties of Oxy-Fluoro Boro Tellurite glasses. Optical Materials. 2020; 109:110368. https://doi.org/10.1016/j.optmat.2020.110368

[48] Kaur R, Bhatia V, Kumar D, Rao SMD, Pal Singh S, Kumar A. Physical, structural, optical and thermoluminescence behavior of Dy2O3 doped sodium magnesium borosilicate glasses. Results in Physics. 2019; 12:827-839. https://doi.org/10.1016/j.rinp.2018.12.005

[49] Lakshminarayana G, Vighnesh KR, Prabhu NS, et al. Dy^{3+}: B_2O_3–Al_2O_3–ZnF_2–NaF/LiF oxyfluoride glasses for cool white or day white light-emitting applications. Optical Materials. 2020; 108:110186. https://doi.org/10.1016/j.optmat.2020.110186

[50] Narasimha Rao N, Naresh P, Raghava Rao P, Swamy BJRSN, Chitti Babu A. Physical and spectroscopic properties of PbO – ZnF2 – B2O3 glasses doped with CuO. Materials Today: Proceedings. 2023; 92:817-822. https://doi.org/10.1016/j.matpr.2023.04.382

[51] Santiago de la Rosa A, Cortés-Hernández DA, Escorcia-García J, López-Herrera HU. White-light luminescence from Tm^{3+}-doped borosilicate glass-ceramics synthesized by the sol-gel route. Ceramics International. 2023; 49(14):23985-23995. https://doi.org/10.1016/j.ceramint.2023.05.002

[52] Sailaja P, Mahamuda S, Swapna K, Venkateswarlu M, Rao AS. Near-infrared photoluminescence studies of neodymium ions doped SrO-Al_2O_3-$BaCl_2$-B_2O_3-TeO2 glasses for laser and fiber amplifier applications. Optics and Laser Technology. 2022; 156:108569. https://doi.org/10.1016/j.optlastec.2022.108569

[53] Ren F, Song C, Cong Y, Wu Y, Bai Y, Zhou D. Near-infrared luminescence enhancement in Yb^{3+}/Ho^{3+} co-doped bismuth-tellurite glass by tailoring glass network. Ceramics International. 2023; 49(20):32850-32859. https://doi.org/10.1016/j.ceramint.2023.07.257

[54] Sharma A, Nazrin SN, Humaira SA, Boukhris I, Kebaili I. Impact of neodymium oxide on optical properties and X-ray shielding competence of Nd_2O_3–TeO_2–ZnO glasses. Radiation Physics and Chemistry. 2022; 195:110047. https://doi.org/10.1016/j.radphyschem.2022.110047

[55] Komal Poojha MK, Naseer KA, Matheswaran P, Marimuthu K, El Shiekh E. Effect of alkali/alkaline modifiers on Pr^{3+} ions doped lead boro-tellurite glasses for lasing material applications. Optical Materials. 2023; 143:114289. https://doi.org/10.1016/j.optmat.2023.114289

[56] Singh J. Optical Properties of Condensed Matter and Applications - Wiley Series in Materials for Electronic - amp - Optoelectronic Applications. 2006.

[57] Ding J, Li C, Xia L, Zhang Y, Li J, Zhou Y. A new Nd^{3+}/Tm^{3+}/Ho^{3+} tri-doped tellurite glass for multifunctional applications. Materials Research Bulletin. 2022; 150:111777. https://doi.org/10.1016/j.materresbull.2022.111777

[58] Shoaib M, Rooh G, Rajaramakrishna R, et al. Comparative study of Sm3+ ions doped phosphate based oxide and oxy-fluoride glasses for solid state lighting applications. Journal of Rare Earths. 2019; 37(4):374-382. https://doi.org/10.1016/j.jre.2018.09.008

[59] Monisha M, D'Souza AN, Hegde V, et al. Dy^{3+} doped SiO_2–B_2O_3–Al_2O_3–NaF–ZnF_2 glasses: An exploration of optical and gamma radiation shielding features. Current Applied Physics. 2020; 20(11):1207-1216. https://doi.org/10.1016/j.cap.2020.08.004

[60] Sasirekha C, Vijayakumar M, Yousef ES, Marimuthu K. Luminescence performance of Dy^{3+} ions incorporated modifier reliant boro-tellurite glasses for white light applications. Optik. 2023; 289:171268. https://doi.org/10.1016/j.ijleo.2023.171268

[61] Ahmadi F, Hussin R, Ghoshal SK. Judd-Ofelt intensity parameters of samarium-doped magnesium zinc sulfophosphate glass. Journal of Non-Crystalline Solids. 2016; 448:43-51. https://doi.org/10.1016/j.jnoncrysol.2016.06.040

[62] Basavapoornima C, Maheswari T, Deviprasad CJ, Kesavulu CR, Tröster T, Jayasankar CK. Thermal, structural, mechanical and 1.8 μm luminescence properties of the thulium doped Pb-K-Al-Na glasses for optical fiber amplifiers. Journal of Non-Crystalline Solids. 2020; 530:119773. https://doi.org/10.1016/j.jnoncrysol.2019.119773